IOP Publishing Journal of Physics: Condensed Matter
J. Phys.: Condens. Matter **27** (2015) 146005 (6pp) doi:10.1088/0953-8984/27/14/146005

Determination of the magnetic structure of $Gd_2Fe_2Si_2C$ by Mössbauer spectroscopy and neutron diffraction

D H Ryan[1], Nadejda Mas[1], R A Susilo[2], J M Cadogan[2] and R Flacau[3]

[1] Department of Physics, McGill University, Montreal, Québec H3A 2T8, Canada
[2] School of Physical, Environmental and Mathematical Sciences, UNSW Canberra at the Australian Defence Force Academy, Canberra, ACT BC 2610, Australia
[3] Canadian Neutron Beam Centre, Chalk River Laboratories, Chalk River, ON K0J 1J0, Canada

E-mail: dhryan@physics.mcgill.ca

Received 2 February 2015, revised 19 February 2015
Accepted for publication 25 February 2015
Published 20 March 2015

Abstract

We have determined the magnetic structure of the intermetallic compound $Gd_2Fe_2Si_2C$ using neutron powder diffraction, ^{155}Gd and ^{57}Fe Mössbauer spectroscopy. This compound crystallizes in a monoclinic ($C2/m$) structure and its magnetic structure is characterized by antiferromagnetic order of the Gd sublattice along the b-axis, with cell-doubling along the c-axis. The propagation vector is $\mathbf{k} = [0\,0\,\frac{1}{2}]$. At 3.6 K the Gd moment reaches 6.2(2) μ_B. Finally, ^{57}Fe Mössbauer spectroscopy shows no evidence of magnetic ordering of the Fe sublattice.

Keywords: Mössbauer spectroscopy, neutron diffraction, magnetic structure, rare earth intermetallics

(Some figures may appear in colour only in the online journal)

1. Introduction

The $R_2Fe_2Si_2C$ (R = rare earth) intermetallic compounds crystallise in a monoclinic structure with the space group $C2/m$ (#12). These compounds are an example of a rare-earth intermetallic series that is stabilised by a small element, in this case carbon, and were discovered in 1988 [1] as a by-product of the search for new permanent magnet materials after the discovery of $Nd_2Fe_{14}B$ and related compounds.

The R, Fe and Si atoms occupy 4i sites with the point symmetry m, generated by (x 0 z). The stabilising C atoms occupy the 2a site (0 0 0), with the point symmetry $2/m$. The magnetic order of the $R_2Fe_2Si_2C$ compounds is antiferromagnetic, with a maximum Néel temperature of 45 K being reported for $Tb_2Fe_2Si_2C$ [2]. On the basis of a neutron diffraction study of $Nd_2Fe_2Si_2C$ and $Tb_2Fe_2Si_2C$ in 1993 [3], it was suggested that the magnetic order in this series involves an antiferromagnetic cell-doubling along the crystal c-axis ($\mathbf{k} = [0\,0\,\frac{1}{2}]$) with both the R and Fe sublattices being ordered, somewhat unusually almost perpendicular to each other.

The Néel temperature of $Gd_2Fe_2Si_2C$ was reported to be 9 K [2] which represents a spectacular failure of the de Gennes scaling, given that the Tb compound orders at 45 K. In a recent report on $Gd_2Fe_2Si_2C$ [4] two quite prominent magnetic signals in magnetometry and susceptibility measurements were observed at 38 K and 58 K although only the lower 'event' was observed in heat capacity measurements. The strong magnetic signal at 58 K was tentatively suggested to represent the magnetic ordering of $Gd_2Fe_2Si_2C$.

Given the ambiguities inherent in these bulk measurements, we have carried out a new determination of the intrinsic magnetism of $Gd_2Fe_2Si_2C$ using the *local* probes of ^{155}Gd and ^{57}Fe Mössbauer spectroscopy, complemented with neutron powder diffraction.

2. Experimental methods

The $Gd_2Fe_2Si_2C$ sample was prepared by arc-melting the high purity elements under an atmosphere of high-purity argon following the procedure outlined by Pöttgen *et al* [5]. The resulting ingot was wrapped in tantalum foil, sealed under vacuum in a quartz tube and annealed at 1000 °C for 2 weeks, followed by water-quenching. Sample characterisation by

Table 1. Crystallographic data (at 298 K) for $Gd_2Fe_2Si_2C$ determined by x-ray powder diffraction.

Atom	Site	Point Symmetry	x	z
Gd	4*i*	*m*	0.548(4)	0.299(8)
Fe	4*i*	*m*	0.214(8)	0.150(14)
Si	4*i*	*m*	0.17(2)	0.72(3)
C	2*a*	2/*m*	0	0
		Monoclinic $C2/m$ (#12)		
$a = 10.6806(8)$ Å	$b = 3.9539(3)$ Å	$c = 6.8155(4)$ Å	$\beta = 129.47(4)^\circ$	
	$R_{Bragg} = 7.3$	$R_F = 8.1$		

Note: Both atomic sites, the 2*a* and the 4*i*, have a *y* positional parameter equal to zero.

x-ray powder diffraction (XRD) was carried out at room temperature using a Rigaku Miniflex600 with Cu-K_α radiation.

Neutron powder diffraction experiments were carried out on the C2 800-wire powder diffractometer (DUALSPEC) at the NRU reactor, Chalk River Laboratories, Ontario, Canada, using a neutron wavelength (λ) of 1.3286(2) Å. A pattern was also collected at 3.6 K with λ = 2.3789(2) Å to confirm that no low-angle peaks had been missed with the shorter wavelength. No extra peaks were found. Diffraction patterns were obtained over the temperature range 3.6–60 K. Natural gadolinium is the strongest neutron absorber in the periodic table and its scattering length is dependent on the neutron energy, as tabulated by Lynn and Seeger [6], from which we derived the scattering length coefficient appropriate to our neutron wavelength ($\lambda = 1.33$ Å, $E = 46.2$ meV), namely 10.5–12.7*i* fm. The sample mounting arrangement for this strongly-absorbing sample is a large-area, flat-plate, as outlined in a previous paper [7] and successfully used by us in neutron diffraction studies of other Gd-based compounds (e.g. [8–10]). The key magnetic reflections in the low temperature diffraction patterns of $Gd_2Fe_2Si_2C$ occurred below $2\theta = 40^\circ$ so no absorption correction was applied, however the data were truncated at this angle to minimise the potential impact of angle-dependent absorption effects.

All diffraction patterns were analysed using the Rietveld method and the *FullProf/WinPlotr* program [11, 12]. The determination of the symmetry-allowed magnetic structures employed Representational Analysis with the *Basireps* program (part of the *FullProf/WinPlotr* suite [11, 12]) and all notation used in our paper follows that used in *Basireps*.

The 50 mCi ^{155}Sm source for the ^{155}Gd Mössbauer work was prepared by neutron activation of $^{154}SmPd_3$. The source and sample (about 450 mg) were mounted vertically in a helium flow cryostat and the Mössbauer drive was operated in sinusoidal mode. The 86.55 keV γ-photons (excited and ground state spins of $\frac{5}{2}$ and $\frac{3}{2}$, respectively) used for ^{155}Gd Mössbauer spectroscopy were isolated from the x-rays emitted by the source with a high-purity Ge detector. The drive system was calibrated using a laser interferometer with velocities cross-checked against both ^{57}Co**Rh**/α-Fe at room temperature and $^{155}SmPd_3$/$GdFe_2$ at 5 K. The ^{57}Fe Mössbauer spectra were obtained using a standard 20 mCi ^{57}Co**Rh** source.

The ^{155}Gd Mössbauer spectra were fitted using a non-linear least-squares minimization routine with line positions and intensities derived from an exact solution to the full Hamiltonian [13]. The ^{57}Fe spectra were doublets so a full Hamiltonian approach is not required as an analytic solution is possible.

3. Results

3.1. X-ray diffraction

The lattice parameters of $Gd_2Fe_2Si_2C$ obtained by refinement of the x-ray diffraction pattern obtained at 298 K and shown in [4] are given in table 1 and are in excellent agreement with the values reported by Paccard and Paccard [1]. Despite numerous attempts, we were unable to avoid the production of small amounts (estimated at less than 2 wt.% based on refinement of the x-ray diffraction pattern) of an impurity phase matching Gd_3C [14] (reported as $GdC_{0.33}$ to reflect the observed range of Gd:C ratios). As we shall see later in section 3.4, there is also a small amount of an Fe-bearing impurity phase which was not detected by XRD but accounted for around 3% of the ^{57}Fe Mössbauer spectral area. On the basis of the measured isomer shift, we tentatively ascribe this to FeSi [15].

3.2. Neutron diffraction

In figure 1 we compare the neutron diffraction patterns obtained at 60 K (paramagnetic) and at 3.6 K (magnetically ordered). We also show the difference between these two patterns, representing the magnetic contribution. It is immediately apparent that the diffraction data are dominated by an intense, purely magnetic peak occurring at $2\theta = 7.3^\circ$ ($d = 10.44$ Å). This peak indexes as (0 0 $\frac{1}{2}$), indicating a cell-doubled antiferromagnetic structure. In figure 2 we show the refinement of the neutron powder diffraction pattern of $Gd_2Fe_2Si_2C$, obtained at 60 K where $Gd_2Fe_2Si_2C$ is paramagnetic and the pattern therefore comprises only nuclear scattering. The refined lattice parameters at 60 K are $a = 10.682(24)$ Å, $b = 3.938(6)$ Å, $c = 6.807(13)$ Å and $\beta = 129.62(14)^\circ$. The conventional *R*-factors for this refinement are $R_{Bragg} = 17.7$ and $R_F = 11.4$. In figure 3 we show the refinement of the neutron powder diffraction pattern of $Gd_2Fe_2Si_2C$, obtained at 3.6 K. The refined lattice parameters at 3.6 K are $a = 10.667(17)$ Å, $b = 3.936(4)$ Å, $c = 6.804(10)$ Å and $\beta = 129.56(11)^\circ$. At this temperature, $Gd_2Fe_2Si_2C$ is magnetically ordered. As mentioned earlier, this pattern is dominated by the intense, purely magnetic peak occurring at $2\theta = 7.3^\circ$ ($d = 10.44$ Å) which indexes as (0 0 $\frac{1}{2}$), indicating a doubling of the cell along the *c*-axis.

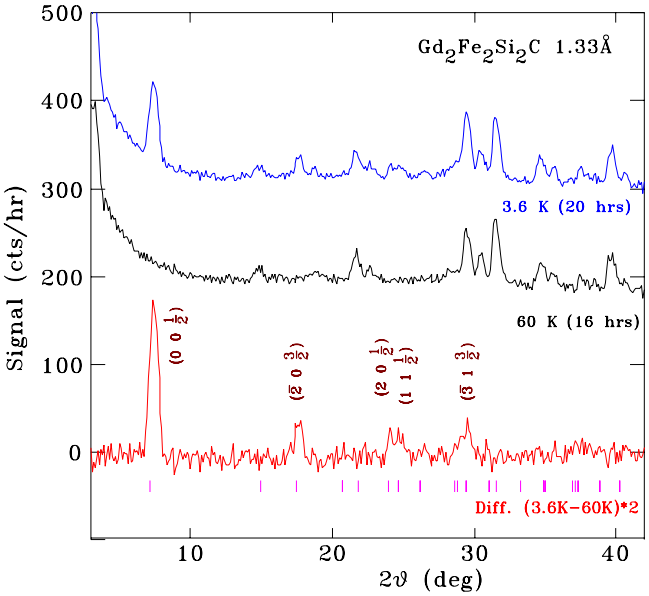

Figure 1. Comparison of the neutron powder diffraction patterns of $Gd_2Fe_2Si_2C$ obtained at 60 K (black, middle) and 3.6 K (blue, top) at a neutron wavelength of $\lambda = 1.3286(5)$ Å. The lowest plot (red) shows the difference between these two patterns (3.6–60 K), scaled up by a factor of 2. A row of Bragg markers shows the positions of the magnetic peaks. The patterns have been displaced vertically for clarity.

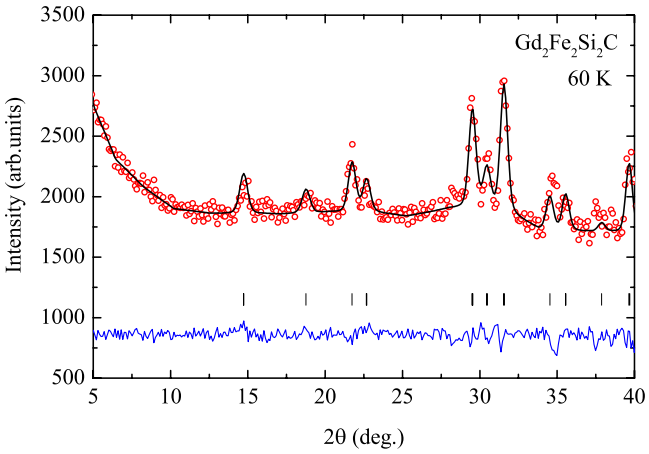

Figure 2. Refined neutron powder diffraction pattern of $Gd_2Fe_2Si_2C$ obtained at 60 K ($\lambda = 1.3286(5)$ Å). The row of Bragg position markers shows the nuclear peaks positions for this $C2/m$ cell.

In order to consider all possible magnetic structures allowed for $Gd_2Fe_2Si_2C$, we carried out Representational Analysis for the Gd $4i$ site (We note here that these representations are also applicable to the Fe which also occupies a $4i$ site). The decomposition of the magnetic representation, for $\mathbf{k} = [0\,0\,\frac{1}{2}]$, comprises four representations:

$$\Gamma^{4i}_{\mathrm{Mag}} = 1\Gamma_1 + 2\Gamma_2 + 2\Gamma_3 + 1\Gamma_4 \qquad (1)$$

and the basis vectors of these irreducible representations are given in table 2. The allowed Gd magnetic order is either b-axial or ac-planar and the best refinement to the 3.6 K neutron diffraction pattern was obtained with the Gd moments aligned

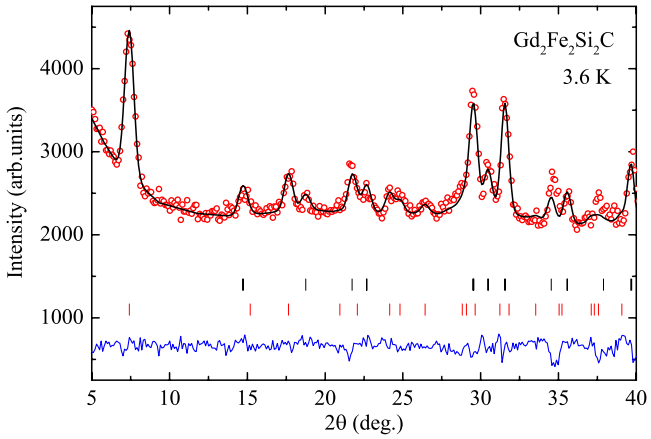

Figure 3. Refined neutron powder diffraction pattern of $Gd_2Fe_2Si_2C$ obtained at 3.6 K ($\lambda = 1.3286(5)$ Å). The two rows of Bragg position markers show the nuclear (top) and magnetic (bottom) peak positions.

Table 2. Representational Analysis for the Gd and Fe $4i$ sites in $Gd_2Fe_2Si_2C$ with a propagation vector $[0\,0\,\frac{1}{2}]$.

Representation	Atom #1 Ordering Mode	Atom #2 Ordering Mode
Γ_1	[0 + 0]	[0 + 0]
Γ_2	[+ 0 +]	[− 0 −]
Γ_3	[+ 0 +]	[+ 0 +]
Γ_4	[0 + 0]	[0 − 0]

Note: The respective basis atomic positions are $(x,\ 0,\ z)$ and $(\overline{x},\ 0,\ \overline{z})$.

antiferromagnetically along the b-axis, corresponding to the Γ_4 representation. The refined Gd magnetic moment at 3.6 K is 6.2(2) μ_B. The conventional R-factors for this refinement are $R_{\mathrm{Bragg}} = 21.4$, $R_{\mathrm{F}} = 14.9$ and $R_{\mathrm{mag}} = 27.6$.

The temperature dependence of the intensity of the purely magnetic $(0\,0\,\frac{1}{2})$ peak is shown in figure 4. A simple fit to these data using a squared $J = 7/2$ Brillouin function, to reflect the variation of magnetic scattering intensity with the square of the magnetic moment, yields a Néel temperature of 37.4(5) K.

3.3. ^{155}*Gd Mössbauer spectroscopy*

In figure 5 we show our set of ^{155}Gd-Mössbauer spectra recorded over the temperature range 5–60 K. At 60 K the ^{155}Gd spectrum is clearly paramagnetic, yielding a quasi-doublet due to the small value of the ratio of the excited state to ground state electric quadrupole moments of the ^{155}Gd nucleus (0.32 b and 1.6 b, respectively). The ground-state electric quadrupole coupling constant eQV_{zz} at 60 K is $-1.13(5)$ mm s^{-1}. Below 40 K the spectrum broadens and eventually a clear magnetic splitting develops. At 5 K, the hyperfine magnetic field at the ^{155}Gd nucleus is 29.6(3) T, the electric quadrupole coupling constant eQV_{zz} is $-1.20(5)$ mm s^{-1} and the electric field gradient asymmetry parameter η is 1.

The temperature dependence of the hyperfine magnetic field at the ^{155}Gd site splitting is shown in figure 6. A simple fit to these data using a $J = 7/2$ Brillouin function, appropriate to the Gd^{3+} $4f^7$ S-state ionic configuration, yields a Néel

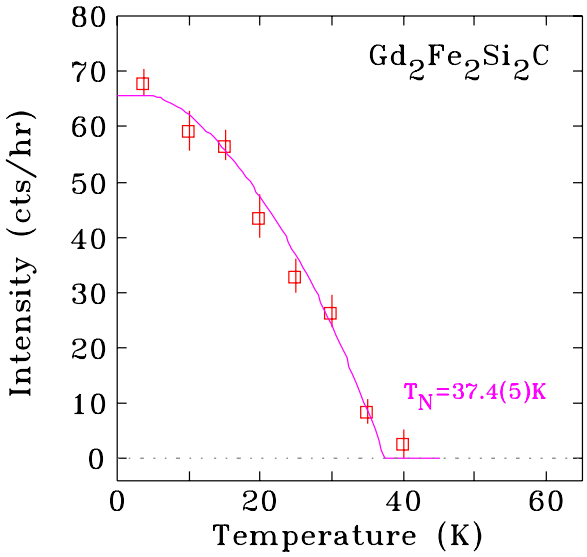

Figure 4. Temperature dependence of the intensity of the $(0\ 0\ \frac{1}{2})$ magnetic peak in $Gd_2Fe_2Si_2C$. The fitted curve is a squared $J = 7/2$ Brillouin function.

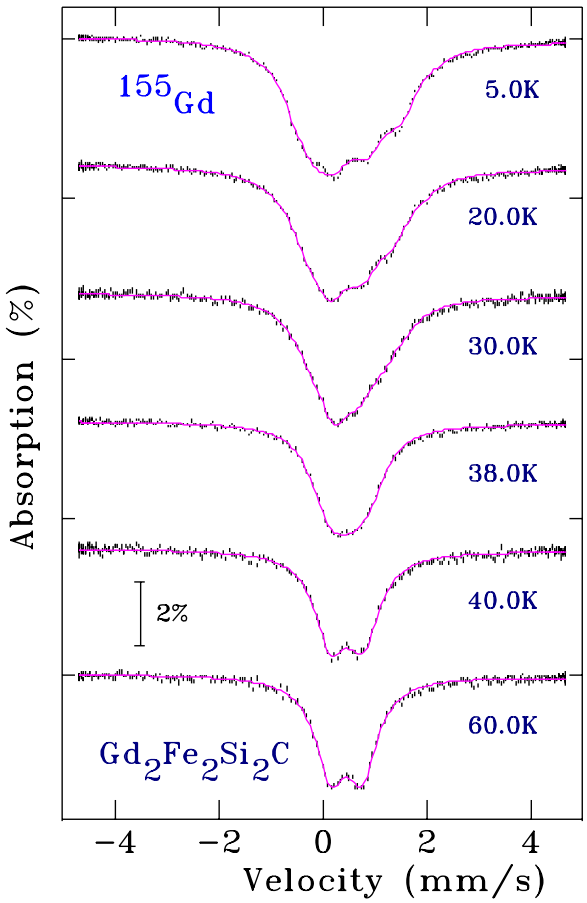

Figure 5. ^{155}Gd Mössbauer spectra of $Gd_2Fe_2Si_2C$ covering the temperature range 5–60 K.

temperature of 38.9(1) K, in very good agreement with the value deduced from our neutron diffraction data. No magnetic splitting is observed above this temperature. It is clear from the use of a direct *local* probe of the Gd magnetic behaviour that the Néel temperature of $Gd_2Fe_2Si_2C$ is 39(1) K which matches the

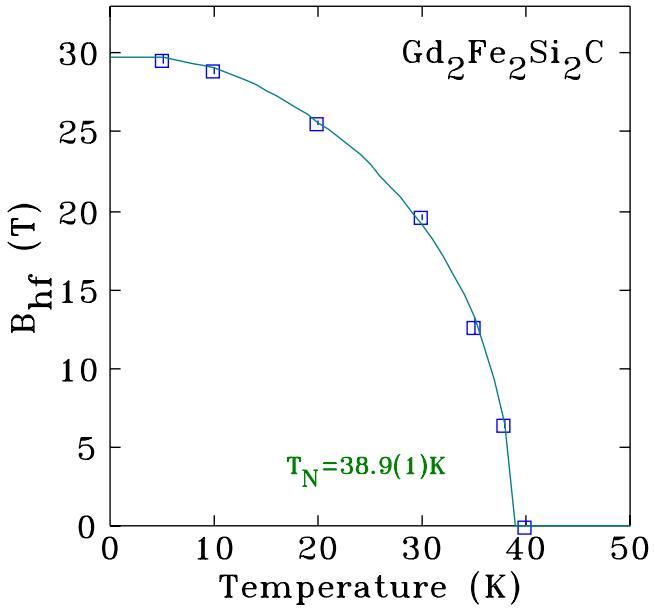

Figure 6. Temperature dependence of the hyperfine magnetic field at the ^{155}Gd nucleus in $Gd_2Fe_2Si_2C$. The fitted curve is a $J = 7/2$ Brillouin function.

specific heat signal previously reported [4]. The strong signal at 58 K seen in ac-susceptibility data [4] does not come from the primary $Gd_2Fe_2Si_2C$ phase and must therefore be due to the presence of a minor ferromagnetic impurity, possibly the Gd_3C phase identified in the previously reported x-ray diffraction pattern [4]. However, since Gd_3C is reported to have a Curie temperature around room temperature [16], if this is indeed the source of the ferromagnetic response seen at 58 K, the phase cannot be stoichiometric.

The normal $J = 7/2$ temperature dependence of both the ^{155}Gd hyperfine field and the intensity of the magnetic scattering at the $(0\ 0\ \frac{1}{2})$ position combined with the ∼30 T hyperfine field measured at 5 K, strongly suggest that gadolinium has a conventional $S = 7/2$, $L = 0$ ground state configuration in $Gd_2Fe_2Si_2C$, and should therefore carry a full $7\,\mu_B$ local moment. We explored the possibility of incommensurate magnetic structures, however these did not lead to improved fits or a larger gadolinium moment. We are left therefore with two possibilities: (i) the reduced Gd moment derived here from the neutron diffraction work reflects a limitation imposed by working with small, highly absorbing samples, or (ii) there is a small moment on the iron atoms that should be included in the fits. The solution serves to emphasise the need to combine data from long-range (neutron diffraction) and local (Mössbauer spectroscopy) probes of the magnetic ordering.

To investigate the possibility that the iron atoms also exhibited an ordered moment, we carried out refinements of the 3.6 K neutron diffraction pattern allowing magnetic moments on both the Gd and the Fe sites and using all combinations of irreducible representations shown in table 2. The fact that both the Gd and the Fe atoms occupy sites of the same symmetry precludes the resolution of the question concerning the possible magnetic order of the Fe. Given the quality of the diffraction data on this highly-absorbing sample, we were able to obtain

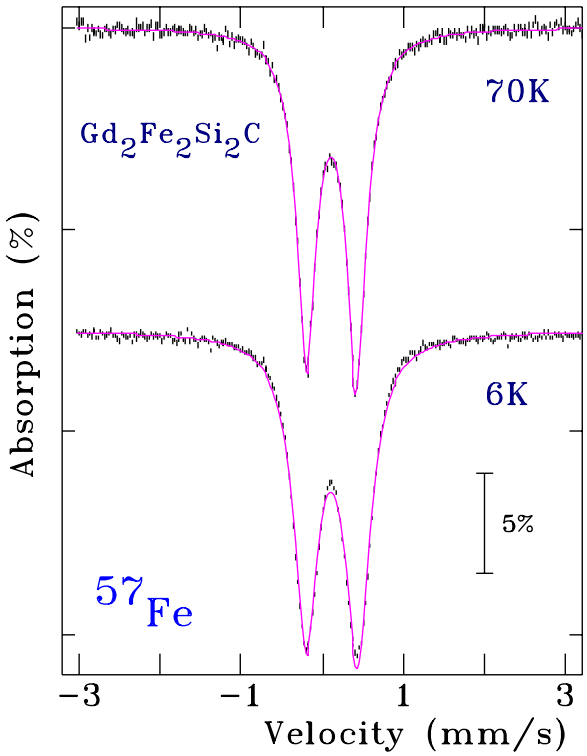

Figure 7. ^{57}Fe Mössbauer spectra of $Gd_2Fe_2Si_2C$ recorded at 70 K and 6 K.

refinements of comparable quality to the Gd-only refinement. However, in all cases the Fe magnetic moment refined to rather large values in the range 2–3 μ_B. In no case did the combined-moment refinements yield a better χ^2 value than the Gd-only refinement. We are therefore forced to conclude that the neutron diffraction data alone are insufficient to resolve the question over the magnetic order of the Fe sublattice. At this point, we turned to another direct, *local* probe of the magnetic behaviour, namely ^{57}Fe Mössbauer spectroscopy.

3.4. ^{57}Fe Mössbauer spectroscopy

In figure 7 we show our ^{57}Fe-Mössbauer spectra recorded at room temperature and at 6 K. The room temperature spectrum is a well resolved quadrupole-split doublet with a quadrupole splitting of 0.575(3) mm s^{-1} and an isomer shift of −0.012(2) mm s^{-1} relative to α-Fe. The slight asymmetry in the doublet is due to an impurity contribution amounting to a relative sub-spectral Mössbauer area of 3%. The isomer shift (relative to α-Fe) of this minor component is 0.40(3) mm s^{-1} and on the basis of the isomer shift and lack of a measurable quadrupole splitting we can rule out potential impurities such as $GdFe_2Si_2$ [17–19], GdFeSi [20–22] and $Gd_2Fe_3Si_5$ [23, 24]. One possibility is FeSi which was reported to have an isomer shift of 0.28 mm s^{-1} and a very small quadrupole splitting [15] and it may be that this minor impurity is FeSi with some incorporated C.

The spectrum acquired at 6 K, well below the magnetic ordering temperature of 39 K, shows no signs of magnetic ordering of the Fe sublattice. It is immediately clear that the Fe is not magnetically ordered and certainly not with a moment

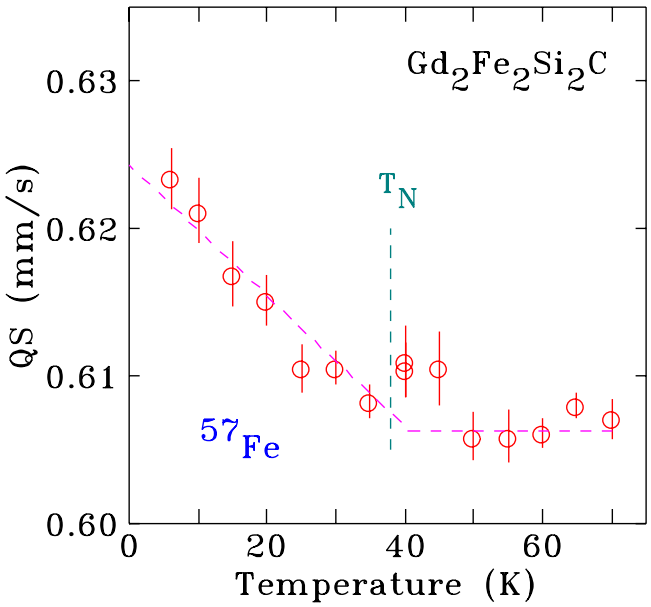

Figure 8. Temperature dependence of the ^{57}Fe quadrupole splitting in $Gd_2Fe_2Si_2C$.

of 2–3 μ_B for which we would expect a hyperfine magnetic field of at least 20 T. To fit our ^{57}Fe spectra we treated them as quadrupole doublets and in figure 8 we show the temperature dependence of this 'effective' quadrupole splitting. The slight increase in splitting below 40 K simply reflects the presence of a very small, unresolvable transferred hyperfine magnetic field at the ^{57}Fe nucleus from the surrounding, magnetically ordered Gd sublattice. We estimate this transferred hyperfine field to be less than 0.5 T.

3.5. Transferred hyperfine field at the ^{57}Fe site

All that remains is to verify that the magnetic structure of the Gd sublattice that we refined from our neutron diffraction data will in fact produce a transferred hyperfine magnetic field at the Fe site in the $Gd_2Fe_2Si_2C$ structure. To this end, we identified the Wigner-Seitz cell around the Fe site using the *Blokje* program [25]. Considering only the magnetic neighbours around the Fe site and using the crystallographic data presented above we find that the Fe site has two Gd neighbours at a distance of 3.09 Å, one at 3.17 Å, one at 3.21 Å and two at 3.24 Å. The respective relative orientations of these neighbouring Gd magnetic moments along the *b*-axis are (− −), (+), (+) and (++) which will produce a transferred hyperfine field at the Fe site. In figure 9 we show the nearest-neighbour environment (only the magnetic Gd atoms) around the Fe site in $Gd_2Fe_2Si_2C$.

3.6. Final thoughts

It seems clear that the use of neutron diffraction alone cannot unequivocally resolve the question over the magnetic order of the Fe sublattice in the $R_2Fe_2Si_2C$ series of intermetallic compounds. The fact that both the R and Fe atoms occupy 4*i* sites, and therefore have the same point symmetry, makes it extremely difficult to distinguish the intrinsic behaviour

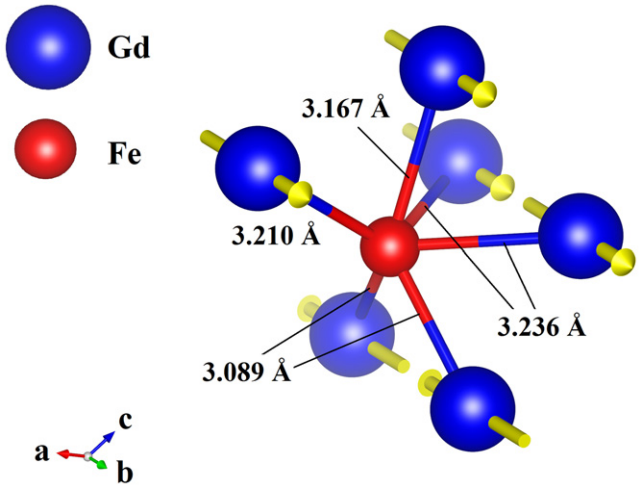

Figure 9. Arrangement of the neighbouring magnetically ordered Gd moments around the Fe site in $Gd_2Fe_2Si_2C$ (drawn using the Vesta software [26]).

of these two potentially magnetically ordered sublattices. However, the use of a direct, *local* probe, in this case Mössbauer spectroscopy, provides definitive evidence that the Fe sublattice in $Gd_2Fe_2Si_2C$ is *not* magnetically ordered. The fact that the Gd ion has the largest spin angular momentum in the rare-earth series leads us to suggest that the Fe sublattice does not order magnetically in any member of the $R_2Fe_2Si_2C$ series. A detailed analysis of the entire intermetallic series, exploiting the complementarity of Mössbauer spectroscopy and neutron diffraction, is clearly warranted and to this end we are currently carrying out new experiments.

4. Conclusions

We have used a combination of ^{155}Gd Mössbauer spectroscopy and neutron powder diffraction to show that the magnetic ordering temperature of the Gd sublattice in $Gd_2Fe_2Si_2C$ is 39(1) K. Below this temperature, the Gd moments are ordered antiferromagnetically along the monoclinic *b*-axis in a cell-doubled arrangement. The propagation vector describing this order is $\mathbf{k} = [0\ 0\ \frac{1}{2}]$. At 3.6 K, the Gd magnetic moment is 6.2(2) μ_B, slightly lower than the 'free-ion' value of 7 μ_B. Finally, to resolve the ambiguity over whether or not the Fe sublattice orders, we carried out ^{57}Fe Mössbauer spectroscopy. We find no evidence for any magnetic order of the Fe sublattice and the slightly increased splitting of the ^{57}Fe spectral lines below the Néel temperature simply reflects a small transferred hyperfine magnetic field at the ^{57}Fe nucleus from the surrounding, magnetically ordered Gd sublattice.

Acknowledgments

We gratefully acknowledge R Rao and R Speranzini for the activation of the ^{155}Gd Mössbauer source in the National Research Universal (NRU) research reactor, which is operated by Atomic Energy of Canada, Ltd., at Chalk River, Ontario. DHR acknowledges support from the Natural Sciences and Engineering Research Council of Canada and Fonds Québécois de la Recherche sur la Nature et les Technologies. JMC acknowledges support from the University of New South Wales. RAS acknowledges a University International Postgraduate Award (UIPA) and a University College Postgraduate Scholarship from the University of New South Wales. Part of this work was carried out during a visit to UNSW Canberra by DHR which was supported by a Rector-funded Visiting Fellowship.

References

[1] Paccard L and Paccard D 1988 *J. Less-Common Met.* **136** 297
[2] Schmitt D, Paccard D and Paccard L 1992 *Solid State Commun.* **84** 357
[3] Le Roy J, Paccard D, Bertrand C, Soubeyroux J. L, Bouillot J, Paccard L and Schmitt D 1993 *Solid State Commun.* **86** 675
[4] Susilo R A, Cadogan J M, Hutchison W D and Campbell S J 2014 *Phys. Status Solidi* A **211** 1087
[5] Pöttgen R, Ebel T, Evers C B H and Jeitschko W 1995 *J. Solid State Chem.* **114** 66
[6] Lynn J E and Seeger P A 1990 *At. Data Nucl. Data Tables* **44** 191
[7] Ryan D H and Cranswick L M D 2008 *J. Appl. Cryst.* **41** 198
[8] Cadogan J M, Ryan D H, Napoletano M, Riani P and Cranswick L M D 2009 *J. Phys.: Condens. Matter* **21** 124201
[9] Ryan D H, Cadogan J M, Cranswick L M D, Gschneidner K A Jr, Pecharsky V K and Mudryk Ya 2010 *Phys. Rev.* B **82** 224405
[10] Cadogan J M, Ryan D H, Mudryk Ya, Pecharsky V K and Gschneidner K A Jr 2014 *J. Appl. Phys.* **115** 17A901
[11] Rodríguez-Carvajal J 1993 *Physica* B **192** 55
[12] Roisnel T and Rodríguez-Carvajal J 2001 *Mater. Sci. Forum* **378–81** 118
[13] Voyer C J and Ryan D H 2006 *Hyp. Int.* **170** 91
[14] Shi J, Izumi H, Machida K and Adachi G 1996 *J. Alloys Compounds* **240** 156
[15] Wertheim G K, Wernick J H and Buchanan D N E 1966 *J. Appl. Phys.* **37** 3333
[16] Takaki H and Mekata M 1969 Structures and physical properties of non-stoichiometric compounds *Meeting of the Japanese Physical Society* (quoted as reference 1 in [14])
[17] Noakes D R, Umarji A M and Shenoy G K 1983 *J. Magn. Magn. Mater.* **39** 309
[18] Umarji A M, Noakes D R, Viccaro P J, Shenoy G K and Aldred A T 1983 *J. Magn. Magn. Mater.* **36** 61
[19] Bara J J, Hrynkiewicz U, Miłoś A and Szytuła A 1990 *J. Less-Common Met.* **161** 185
[20] Welter R, Venturini G and Malaman B 1992 *J. Alloys and Compounds* **189** 49
[21] Welter R 1994 *PhD Thesis* Université Henri Poincaré—Nancy I, France
[22] Napoletano M, Canepa F, Manfrinetti P and Merlo F 2000 *J. Mater. Chem.* **10** 1663
[23] Braun H F, Segre C U, Acker F, Rosenberg M, Dey S and Deppe P 1981 *J. Magn. Magn. Mater.* **25** 117
[24] Noakes D R, Shenoy G K, Niarchos D, Umarji A M and Aldred A T 1983 *Phys. Rev.* B **27** 4317
[25] Gelato L 1982 *J. Appl. Cryst.* **14** 151
[26] Momma K and Izumi F 2011 *J. Appl. Cryst.* **44** 1272